Research Square

Preprints are preliminary reports that have not undergone peer review.
They should not be considered conclusive, used to inform clinical practice,
or referenced by the media as validated information.

Developmental Timing of Neonatal Inflammatory Pain Differentially Alters Adult Dentate Gyrus Plasticity in Male Wistar Rats

Laura N. C. Braga
Federal University of São João del-Rei
Gisele S. Nogueira
Federal Institute of Minas Gerais
Arthur C. Pires
Federal University of São João del-Rei
Antônio M. Rodrigues
amr@ufsj.edu.br

Federal University of São João del-Rei
Carla A. Scorza
Federal University of São Paulo
Fulvio A. Scorza
Federal University of São Paulo
Luciene Covolan
Federal University of São Paulo
Antônio-Carlos G. Almeida
Federal University of São João del-Rei

Research Article

Keywords: brain-derived neurotrophic factor (BDNF), long-term potentiation (LTP), Morris water maze, neonatal pain, newborn nociception, plasticity

Posted Date: September 30th, 2026

DOI: https://doi.org/10.21203/rs.3.rs-10840537/v1

License: This work is licensed under a Creative Commons Attribution 4.0 International License.
Read Full License

Additional Declarations: No competing interests reported.

Abstract

Preterm newborns in neonatal intensive care units are frequently exposed to painful procedures, raising concerns about their neurodevelopmental impact. We investigated whether neonatal inflammatory nociceptive stimulation produces persistent alterations in adult hippocampal function. Male Wistar rat pups received Complete Freund's Adjuvant in the left hind paw on postnatal day 1 (P1) or 8 (P8). The study focused on long-term potentiation (LTP) and excitability in the adult dentate gyrus, complemented by Morris water-maze performance and hippocampal brain-derived neurotrophic factor (BDNF) as a functional assessment and molecular corroboration, respectively. Hippocampal IL-6, IL-10, and TNF-α were used to assess persistent inflammation, and thermal sensitivity contextualized the model. Electrophysiological effects were layer- and parameter-specific: P1 showed greater normalized slope potentiation in the granule-cell layer but lower normalized EPSP and slope potentiation in the molecular layer than CTR; P8 showed increased population-spike-related measures and lower normalized molecular-layer slope potentiation than CTR. P1 and P8 had shorter escape latencies than CTR on training days 3 and 4, whereas probe-trial performance did not differ. Both stimulated groups showed increased BDNF and reduced thermal sensitivity. No cytokine increases indicative of sustained hippocampal inflammatory activation were detected; at P30, IL-6 and IL-10 were lower in P1 than in age-matched controls. Thus, neonatal inflammatory pain was associated with persistent, developmental-stage-dependent modification of adult dentate gyrus plasticity, supported by concurrent functional and molecular findings without evidence of increased hippocampal IL-6, IL-10, or TNF-α up to P30.

Introduction

Preterm newborns in neonatal intensive care units (NICUs) often undergo numerous invasive procedures (Fitzgerald et al. 1988; Anand 1998). According to Bhutta et al. (2001), preterm infants average 14 daily invasive procedures. Evidence suggests that repeated early-life exposure may induce long-lasting changes in nociceptive processing (Grunau et al. 2006; Walker et al. 2004; Lidow 2002; Malheiros et al. 2024; Rêgo et al. 2022). These findings underscore the importance of studying early-life nociceptive experiences on CNS development.

The nociceptive circuitry becomes functionally active in late gestation, enabling premature newborns to respond to painful and non-painful stimuli (Anand and Carr 1989). Clinical and preclinical studies consistently show that early-life pain exposure induces lasting changes in somatosensory processing (Lima et al. 2014; LaPrairie and Murphy 2010; Ren et al. 2004). Children born preterm or at term with NICU experience often exhibit altered pain sensitivity, which may persist into adolescence (Adamson et al. 1991; Unruh 1996).

Rodents, particularly neonatal rats, are widely used as models of neonatal pain because their behavioral and neurodevelopmental features resemble those of human infants (Guy and Abbott 1992; Johnston et al. 1993; Anand et al. 1999). In rodents, neonatal nociceptive stimulation induces long-lasting changes in somatosensory function (Bernardi 1986; Grunau et al. 2007), increases hippocampal neurogenesis

(Malheiros et al. 2024; Lima et al. 2014), alters pain-related brain activation (Malheiros et al. 2021), heightens anxiety- (Rêgo et al. 2022) and depressive-like behaviors (Negrigo et al. 2011) and modifies hippocampal 5-HT_{1A} receptor and p-CREB expression (Rêgo et al. 2022). Collectively, these findings highlight the importance of clarifying how neonatal pain disrupts processes relevant to learning and memory (Amaral et al. 2015).

Long-term potentiation (LTP) is an experimental model for studying synaptic plasticity and its role in learning and memory (Bliss and Collingridge 1993; Cooke and Bliss 2006). Chronic stress in adulthood impairs hippocampal LTP in rodents (Kim et al. 1996; Joëls et al. 2004; Pavlides et al. 2002), a critical region for cognitive and emotional functions (Lupien et al. 2009). Evidence shows neonatal nociceptive stimulation impairs adult spatial memory (Negrigo et al. 2011) despite increasing neurogenesis (Lima et al. 2014; Lupien et al. 2009; Malheiros et al. 2014). This supports the hypothesis that early-life stress results in long-term structural/functional changes in the hippocampus, particularly during rapid peri- and postnatal development (Leslie et al. 2011; Altman and Das 1965; Brunson et al. 2005). Thus, using LTP protocols provides insights into how early nociceptive experiences influence CNS plasticity and development.

This study tested whether the developmental timing of neonatal inflammatory nociceptive stimulation produces persistent changes in adult dentate gyrus function, with a focus on LTP and excitability. Morris water-maze performance provided a functional assessment, and hippocampal BDNF served as a molecular marker of long-term neurodevelopmental alterations, highlighting a persistent association between early nociceptive experiences and adult neurotrophic expression. Hippocampal IL-6, IL-10, and TNF-α were measured as interpretive controls for persistent inflammation, while thermal sensitivity contextualized the long-term sensory consequences of the neonatal CFA model.

Materials and Methods

Subjects and noxious stimulation

Animals

All procedures were conducted following approval from the Ethics Committee of the Universidade Federal de São João del Rei (Protocol No. 024/2016), and all efforts were made to minimize animal suffering. Timed-pregnant Wistar rats were acquired on gestational day 14 from the Center for Development of Animal Models at the Universidade Federal de São Paulo. The dams were housed individually in plastic cages maintained in a temperature-controlled environment (23 ± 2°C), with adequate ventilation and a 12-hour light–dark cycle (lights on at 7:00 AM). Animals had ad libitum access to food (Nuvilab®) and water throughout the study. The day of birth was designated as postnatal day 0 (P0), with subsequent days labeled accordingly through P90.

Neonatal CFA model

Noxious stimulation was induced by a subcutaneous intraplantar injection of 25 µL Complete Freund's Adjuvant (CFA; Sigma-Aldrich, F5881). The commercial suspension contains 1 mg/mL heat-killed and dried Mycobacterium tuberculosis H37Ra, 0.85 mL/mL paraffin oil, and 0.15 mL/mL mannide monooleate. For this study, CFA was first prepared at 25% (v/v) in saline and then diluted 1:2 with saline immediately before administration, yielding a final 12.5% (v/v) CFA preparation. Injections were administered on either P1 or P8, delivered slowly into the plantar surface of the left hind paw using a sterile 29G insulin syringe as previously published (Lima et al. 2014). This procedure produced a local inflammatory nodule, which typically lasted for approximately one week, as previously reported as an experimental model of persistent pain (Ruda et al. 2000). Each pup was gently removed from the cage, separated from the dam and littermates, and placed on a soft absorbent surface. The entire handling and injection process was completed in under one minute per animal to minimize stress. Immediately following CFA injection, each pup was closely monitored during the brief post-injection period before being returned to the home cage. The occurrence and general pattern of expected nocifensive responses, including paw licking, vocalizations, limb shaking, and spinning, were noted qualitatively as part of routine animal welfare monitoring. These observations were intended to confirm recovery and identify any unexpected or excessive reaction to the procedure; they were not defined as experimental behavioral outcomes. Consequently, no predefined latency, duration, frequency, or severity scores were assigned, and no individual quantitative dataset suitable for statistical analysis was generated. All pups recovered from the procedure and were returned to the dam. Control animals underwent the same handling and brief maternal separation as the CFA-exposed groups but received no intraplantar injection, ensuring comparable exposure to handling-related stress. This condition was selected to compare neonatal inflammatory nociceptive stimulation with the absence of an invasive neonatal insult, because intraplantar saline injection may itself produce local tissue injury and transient inflammation. Previous work found no differences in subsequent nociceptive responses between neonatally saline-injected and untreated rats (Hohmann et al. 2005).

All animals were weighed weekly using a precision digital scale (0.1 g accuracy), starting on P1 (Fig. 1a). Animals weighing less than 5 g on P1 were excluded due to their reduced likelihood of survival following experimental manipulation. Pups were weaned on P21 and subsequently housed in groups of five per cage, according to experimental condition. To determine whether inflammatory alterations remained detectable after neonatal CFA exposure, additional subsets of animals were euthanized at the specified post-neonatal time points. The following experimental groups were established: P1-D4, P1-D30, P8-D11, P8-D30, CTR-D4, CTR-D11, and CTR-D30. Exact analyzable sample sizes are reported in the Results and Fig. 2 legend.

Following neonatal treatment, 45 male rats comprised the adult experimental cohort. Only male rats were included to maintain comparability with previous datasets generated using the same neonatal CFA paradigm (Malheiros et al. 2014; Amaral et al. 2015). Beginning at P60, subsets of these animals underwent behavioral assessment using the hot-plate test and Morris water maze. Between P75 and P90, animals were euthanized by decapitation, and hippocampal tissue was collected for ex vivo

electrophysiological recordings and/or BDNF quantification. Endpoint-specific sample sizes are reported in the Results and/or corresponding figure legends.

Experimental design

Animals were assigned to the CTR, P1, and P8 groups using random selection within each litter to minimize bias. Only one animal per litter was allocated to the same treatment group, thereby controlling for potential litter effects. All procedures involving behavioral tests, tissue processing, slice selection, and electrophysiological recordings were performed by experimenters blinded to the neonatal treatment condition until completion of data acquisition and quantification. During experiments, slices and animals were coded numerically, and the experimenter was unaware of group identity. Statistical analyses were performed using datasets in which treatment labels remained coded until all measurements and exclusions were finalized. This combination of within-litter randomization, restriction on litter representation, and blinded data collection and analysis ensured that treatment effects were not confounded by litter-related variability or experimenter bias.

The outcome hierarchy centered on dentate gyrus LTP and excitability. Morris water-maze performance and hippocampal BDNF served as functional and molecular corroboration, respectively; hippocampal cytokines assessed whether inflammatory alterations remained detectable up to P30; and hot-plate sensitivity contextualized the model. Behavioral endpoints were evaluated in endpoint-specific cohorts. The hot-plate test included 10 CTR, 11 P1, and 12 P8 animals. The Morris water maze initially included 12 CTR, 11 P1, and 10 P8 animals. Two CTR and one P1 animal were excluded because marked agitation and stress responses prevented valid task performance, resulting in 10 animals per group for the MWM analyses. Sample sizes were informed by previous studies using the same neonatal CFA model and by the number of independent animals meeting the experimental and recording-quality criteria. A prospective power calculation was not performed because directly comparable estimates of effect size and variability were unavailable for the layer- and parameter-specific dentate gyrus electrophysiological outcomes examined here.

Hippocampal electrophysiology

Electrophysiological evaluations of hippocampal function were conducted between P75 and P90. Animals were euthanized by decapitation using a guillotine. Following a longitudinal scalp incision and bilateral cranial cuts, the upper portions of the skull were removed to expose the brain. The exposed brain was immediately bathed in ice-cold, modified Ringer's solution (127 mM NaCl, 2 mM KCl, 1.5 mM $MgSO_4$, 1.1 mM KH_2PO_4, 26 mM $NaHCO_3$, 2 mM $CaCl_2$, and 10 mM glucose) to reduce metabolic activity and minimize excitotoxicity. The brain was then carefully extracted with a spatula and submerged in semi-frozen Ringer's solution. Hippocampi were dissected and sectioned into 400 µm-thick coronal slices using a chopper-type tissue slicer. Slices from the middle third of the hippocampus were selected and initially maintained in a perfusion chamber filled with continuously oxygenated Ringer’s solution for

3 hours to allow for recovery. One slice per animal was included in the statistical analysis. Afterward, the slices were transferred to an interface recording chamber, placed on filter paper, and perfused with oxygenated Ringer's solution at 31°C, continuously bubbled with a gas mixture of 95% O_2 and 5% CO_2.

For stimulation, we used a bipolar blunted tip tungsten electrode, with an outer pole diameter of 75 µm. Extracellular field potentials were recorded using borosilicate glass micropipettes (World Precision Instruments, USA) pulled to a tip resistance of 2–4 MΩ when filled with Ringer's solution. The recording electrodes were positioned under visual guidance in either the suprapyramidal granule cell layer or the molecular layer. Signals were amplified using a differential AC amplifier (Axonclamp 900A), low-pass filtered at 2 kHz, digitized at 10 kHz using a National Instruments A/D converter controlled by custom acquisition software. Electrode characteristics and configuration were chosen to optimize the spatial resolution of population EPSPs and population spikes, and to ensure reproducibility of dentate gyrus (DG) LTP recordings.

For electrophysiological recordings, the stimulating electrode was positioned in the perforant path, and the recording electrode was placed in the suprapyramidal blade of the DG, targeting the granule cell or molecular layer (Fig. 1b). Initial 10 V pulses were delivered to verify electrode placement and signal quality. In our system, which uses voltage rather than current-controlled stimulation, a 10 V pulse results in currents well within the physiological range used during the subsequent input–output curve. This procedure has been routinely employed in our laboratory (Almeida et al. 2008; Covolan et al. 2014) and has been shown not to compromise slice viability or LTP induction. Following this validation step, the stimulation intensity was immediately reduced, and a full input–output curve (1–18 V) was generated to determine the 50% maximal response, which was subsequently used for baseline recordings. The formal stimulation protocol began with biphasic pulses (100 µs total duration: 50 µs positive phase, 50 µs negative phase), starting at 1.0 V and increasing in 1.0 V increments up to 18.0 V (Fig. 1c), with 30-second intervals between stimuli. The maximum evoked response amplitude was determined, and a stimulation voltage corresponding to 50% of this maximum was identified for use in subsequent recordings. Baseline responses were recorded at 60-second intervals using 50% maximal stimulus intensity for approximately 20 minutes, until the signal stabilized (Fig. 1d). Long-term potentiation (LTP) was then induced using a high-frequency stimulation (HFS) protocol - specifically, a theta-burst stimulation (TBS) pattern (Fig. 1e). This consisted of 10 trains of pulses with 0.25-second intervals; each train contained 5 stimuli delivered at 100 Hz (10 ms interstimulus interval). Following HFS, evoked responses were again recorded every 60 seconds for approximately one hour to assess post-tetanic potentiation and LTP compared to the pre-HFS baseline (Almeida et al. 2008; Covolan et al. 2014).

Alterations in LTP were assessed from extracellular field-potential recordings (Fig. 1e) by quantifying three measures (Bronzino et al. 1994; Bliss and Lomo 1973): excitatory postsynaptic potential (EPSP), slope, and the population spike (PS) amplitude. The EPSP was computed as the difference between the peak of the evoked response and the pre-stimulus baseline. The slope parameter was obtained as the coefficient of a linear regression fitted to the initial rising phase (Fig. 1e). For the PS, a local baseline during the spike was defined by fitting a straight line through the two deflection peaks that bracket the

PS (Fig. 1e); the PS amplitude was then calculated as the vertical distance between the PS peak and the value of this baseline. For the LTP analyses in which parameters were normalized, normalization was performed relative to the pre-HFS baseline values. Specifically, for each slice, the mean of the last 15 minutes of recordings before HFS was calculated, and all post-HFS values were expressed as a percentage of this baseline. Thus, normalization was carried out within each slice, using its own baseline as the reference.

Morris water maze

A black round fiberglass pool, 170 cm in diameter and 50 cm high, was filled to a depth of 25 cm with water (temperature: 26 ± 1°C). A transparent acrylic platform (9 cm diameter), mounted on a transparent support, was placed in the center of the northeast quadrant, 1–2 cm below the surface. The poolroom measured 3.2 · 4.5 m and had several salient visual cues on the walls. In each swimming trial, rats were placed in the water facing the wall of the pool at one of the following locations: south, southeast, east, or northeast, at random. The animal was then allowed to swim until it found the hidden platform. If the rat did not find the platform within 60 s, it was manually guided to it, where the animal remained for 15 s.

Each rat underwent a training phase consisting of four swimming trials/day for 4 consecutive days, with a 30 min intertrial interval. During the training phase, the escape platform remained fixed in the same quadrant. Twenty-four hours after the final training phase, the platform was removed. Rats were randomly placed in the pool and allowed to swim for 60 s. The time spent in the northeast quadrant was recorded. Scoring in both MWM was conducted from video-recorded sessions using Ethovision (Noldus, Wageningen, The Netherlands).

Hippocampal BDNF

Following brain removal, one hippocampus was used for electrophysiological slice preparation, whereas the contralateral hippocampus was immediately homogenized for BDNF quantification in 0.01 M Tris hydrochloride (pH 7.6) containing 5.8% of sodium chloride, 10% of glycerol, 1% of Nonidet P40 (NP-40), 0.4% of ethylenediamine tetraacetic acid (EDTA) and protease inhibitors. Samples were sonicated and stored at -80˚C. Hippocampal BDNF concentrations were quantified in 7 CTR, 8 P1, and 8 P8 animals. CTR animals had not received neonatal CFA stimulation. Hippocampal BDNF concentration assays were performed using the ELISA kit E-maxVR (Promega) according to the manufacturer's recommendations. Samples were thawed and centrifuged for 5 min at 14,000 rpm at 4˚C; the supernatant was transferred to a 96-well plate (Corning Costar) coated with anti-BDNF (1:1000) then incubated for 2 h at room temperature. After this period, the plate was washed with Tris-buffered saline Tween-20 (TBS-T) and incubated with the following antibodies: anti-human (1:500) for 2 h, and conjugate anti-IgY HRP (1:200) for 1 h. After these procedures, color reaction with tetramethyl benzidine was quantified in a plate reader at 450 nm (Quick Elisa). Values are reported in pg/ml.

Cytokine quantification

For cytokine detection, the right hippocampus was homogenized in 0.01 M Tris-hydrochloride buffer (pH 7.6) containing 5.8% sodium chloride, 10% glycerol, 1% Nonidet P-40 (NP-40), 0.4% ethylenediaminetetraacetic acid (EDTA), and protease inhibitors. Samples were sonicated, centrifuged at 10,000 ×g for 5 min at 4°C, and the supernatants were stored at − 80°C until analysis.

Cytokine concentrations were determined using a Millipore multiplex Rat Cytokine Magnetic Bead Panel (RECYTMAG-65K) analyzed on the Luminex® 200™ platform (xPonent/Analyst Software version 4.2). Longitudinal controls were included to assess inter-assay variability. Cytokine concentrations were expressed as pg/mL.

To evaluate whether neonatal CFA exposure induced persistent central inflammatory activation, hippocampal levels of IL-6, IL-10, and TNF-α were quantified 3 days after nociceptive stimulation and on postnatal day 30. The 30-day time point was selected to assess whether inflammatory alterations persisted beyond the acute neonatal response and after the expected resolution of the local peripheral inflammatory process. Cytokine measurements were not extended to later adult ages, including P79, because the primary objective was to determine whether sustained inflammatory activation remained detectable during the post-neonatal developmental period following CFA exposure.

Hot plate

The nociceptive test consisted of placing the rat on a hot plate (52.5°C) and measuring the latency for paw withdrawal. To avoid potential tissue damage, a 20 s automatic termination of the heat stimulus was established if no paw withdrawal occurred. This cut-off time (20 s) was then considered as the maximal latency. The hot plate test data were averaged from three trials with 15 min intervals. The testing apparatus was cleaned between sessions. The observer was blind to treatment during testing.

Statistical analysis

Data are presented as mean ± SEM. Hot-plate, probe-trial, and BDNF data were analyzed using one-way analysis of variance (ANOVA). Significant hot-plate and BDNF effects were followed by pooled-variance pairwise comparisons with Bonferroni adjustment. Morris water-maze acquisition was evaluated using group comparisons conducted separately on each training day; the four day-specific ANOVAs were adjusted by the Holm method, and significant days were followed by pooled-variance pairwise comparisons with Bonferroni adjustment across the six comparisons performed on days 3 and 4. Because the cytokine datasets had small sample sizes, multiple zero values, and asymmetric distributions, age-matched cytokine comparisons were analyzed nonparametrically. CTR-D4 versus P1-D4 and CTR-D11 versus P8-D11 were compared using two-sided Mann–Whitney tests with exact permutation P values. At D30, CTR-D30, P1-D30, and P8-D30 were compared using the Kruskal–Wallis test followed, when significant, by Dunn–Bonferroni post hoc comparisons. Electrophysiological data

were analyzed using nonparametric statistics because EPSP slope, EPSP amplitude, and PS amplitude did not satisfy the assumptions of normality or homogeneity of variance, as determined by the Shapiro–Wilk and Levene tests. Group differences were analyzed using the Kruskal–Wallis test, followed by Dunn–Bonferroni post hoc comparisons when appropriate. Differences in population-spike occurrence among the CTR, P1, and P8 groups were evaluated using the Fisher–Freeman–Halton exact test for 3 × 2 contingency tables. Cramér's V was calculated as an exploratory effect-size estimate. Statistical comparisons were conducted at t = − 15 min (before HFS) for non-normalized data and at t = 55 min (after HFS) for normalized and non-normalized LTP data. Significance was set at $P < 0.05$. Temporal cytokine changes were analyzed separately within each experimental condition. CTR-D4, CTR-D11, and CTR-D30 were compared using the Kruskal–Wallis test followed by Dunn–Bonferroni comparisons; P1-D4 versus P1-D30 and P8-D11 versus P8-D30 were compared using two-sided Mann–Whitney tests with exact permutation P values. To control multiplicity across related omnibus tests, the Benjamini–Hochberg procedure was applied at a 5% false-discovery rate to four biologically defined families: normalized electrophysiological outcomes (EPSP and slope in the granule-cell and molecular layers; four tests), absolute electrophysiological outcomes (EPSP, slope, and PS at − 15 and 55 min in both layers; 12 tests), adult behavioral endpoints (hot-plate and probe trial; two tests), and age-matched cytokine outcomes, evaluated separately at D4, D11, and D30 (three cytokines per age). BDNF was treated as a single molecular endpoint. FDR-adjusted values are reported as q values. Post hoc contrasts were interpreted only when the corresponding omnibus test remained significant after FDR adjustment; Dunn–Bonferroni P values were not subjected to a second adjustment. Temporal cytokine comparisons remained exploratory and were not included in these multiplicity-control families. For ANOVA, partial eta squared (ηp^2) is reported as an omnibus effect-size estimate.

Results

Dentate gyrus LTP and excitability

Hippocampal LTP in the Dentate Granular Layer

In the granule-cell layer, HFS increased normalized EPSP and slope values in all groups (Fig. 2). At 55 min, slope potentiation was greater in P1 than in CTR and P8, whereas normalized EPSP did not differ among groups. CTR and P8 did not differ in slope, indicating a selective increase in slope potentiation after P1 stimulation.

Absolute EPSP and slope values did not differ among groups before or 55 min after HFS (Fig. 3). PS amplitude differed at baseline ($H(2) = 7.270$, $P = 0.0264$, $q = 0.0396$), with P8 higher than P1, and after HFS ($H(2) = 10.195$, $P = 0.0061$, $q = 0.0122$), with P8 higher than CTR and P1. The remaining comparisons were nonsignificant. Population spikes were descriptively more frequent in P8 (6/8, 75.0%) than in CTR (3/8, 37.5%) or P1 (2/7, 28.6%); however, population-spike occurrence did not differ significantly among groups according to the Fisher–Freeman–Halton exact test ($P = 0.1953$; exploratory Cramér's $V = 0.404$).

Hippocampal LTP in the Dentate Molecular Layer

In the molecular layer, population spikes occurred in 5/9 P8 (55.6%), 3/7 P1 (42.9%), and 1/6 CTR (16.7%) recordings, with no statistically significant difference in occurrence among groups (Fisher–Freeman–Halton exact test, p = 0.474; Fig. 4). At 55 min, normalized EPSP differed among groups (H(2) = 7.140, P = 0.0282, q = 0.0376), with greater potentiation in CTR than P1 but no significant CTR–P8 difference. Normalized slope also differed (H(2) = 7.911, P = 0.0192, q = 0.0376), with CTR greater than both P1 and P8. Thus, P1 stimulation was associated with lower normalized EPSP and slope potentiation than CTR, whereas P8 was associated with lower normalized slope potentiation. These comparisons describe relative changes from each slice's own baseline and should be considered together with the absolute baseline responses reported below.

Absolute EPSP, slope, and PS differed among groups before and after HFS (Fig. 5). At baseline, P8 had higher EPSP than CTR and P1, higher slope than CTR, and higher PS than CTR and P1. At 55 min, P8 had higher EPSP and slope than P1 and higher PS than CTR; all other pairwise comparisons were nonsignificant. These effects were therefore parameter- and comparison-specific, with no significant CTR–P1 difference.

Morris water maze

Mean escape latency decreased across training days in all groups (Fig. 6a). Day-specific comparisons were nonsignificant on days 1 and 2 but significant on days 3 and 4, when CTR had longer latencies than P1 and P8; P1 and P8 did not differ (complete statistics in Fig. 6a). Probe-trial performance did not differ among groups ($F[2,27] = 0.225$, $P = 0.800$, $q = 0.800$; $\eta p^2 = 0.016$), providing no evidence of a difference in long-term spatial-memory retrieval.

Hippocampal BDNF

Hippocampal BDNF differed among groups ($F[2,20] = 45.77$, $P < 0.0001$; $\eta p^2 = 0.821$; single molecular endpoint; Fig. 6b). Concentrations were higher in P1 and P8 than in CTR (both Bonferroni-adjusted $P < 0.0001$) and higher in P8 than P1 ($P = 0.0012$), showing an age-dependent association between neonatal stimulation and adult BDNF levels.

Thermal sensitivity

Paw-withdrawal latency differed among groups ($F[2,30] = 11.26$, $P = 0.00023$, $q = 0.00046$; $\eta p^2 = 0.429$) and was greater in P1 (13.03 ± 1.10 s; Bonferroni-adjusted $P = 0.019$) and P8 (15.85 ± 1.00 s; $P = 0.00015$) than in CTR (8.18 ± 1.37 s). P1 and P8 did not differ ($P = 0.256$), indicating reduced thermal sensitivity in both stimulated groups (Fig. 6c).

Hippocampal cytokines

No age-matched CFA-related differences in IL-6, IL-10, or TNF-α were detected at D4 or D11 after FDR adjustment (all $q > 0.05$; Fig. 7). At D30, group effects remained significant after FDR adjustment for IL-6 ($H(2) = 7.511$, $P = 0.0234$, $q = 0.0458$) and IL-10 ($H(2) = 6.980$, $P = 0.0305$, $q = 0.0458$), but not TNF-α ($H(2) = 2.842$, $P = 0.2414$, $q = 0.2414$). Dunn–Bonferroni tests showed lower IL-6 ($P = 0.0390$) and IL-10 ($P = 0.0410$) in P1-D30 than in CTR-D30; the other D30 comparisons were nonsignificant. Thus, no cytokine increase indicative of sustained hippocampal inflammation was detected, although P1 stimulation was associated with lower IL-6 and IL-10 at D30. Given the modest samples and multiple comparisons, these findings are exploratory. Temporal analyses identified developmental changes in all three cytokines in controls, lower TNF-α at D30 than D4 in P1, and higher IL-6 and IL-10 at D30 than D11 in P8; complete statistics are reported in Fig. 7.

Discussion

The primary finding is that neonatal inflammatory nociceptive stimulation produced persistent, developmental-stage- and layer-dependent changes in adult dentate gyrus LTP and excitability. Morris water-maze performance provided a functional assessment, hippocampal BDNF provided molecular corroboration, and the cytokine profile constrained interpretation by showing no persistent increase in hippocampal IL-6, IL-10, or TNF-α. Longer hot-plate withdrawal latencies contextualized the model by demonstrating a lasting sensory consequence. This hierarchy centers the interpretation on dentate physiology while using behavioral and molecular outcomes as convergent support. Persistent effects of early-life adversity on neuronal function provide the broader framework for this interpretation (Anand and Scalzo 2000; Beggs et al. 2012; Brunson et al. 2001; Schneiderman et al. 2003; Zoghbi and Bear 2012).

The effects depended on developmental timing. In the granule-cell layer, P1 enhanced normalized slope potentiation relative to CTR and P8, whereas normalized EPSP did not differ among groups. Conversely, normalized molecular-layer slope potentiation was lower in both stimulated groups than in controls, while normalized EPSP potentiation was lower only in P1 than in CTR. Because baseline molecular-layer responses differed among groups, these normalized differences should be interpreted in conjunction with the corresponding absolute responses. The distinct P1 and P8 profiles suggest developmentally sensitive windows rather than a uniform consequence of neonatal inflammation. Differences between these ages in hippocampal maturation, microglial and neuroimmune signaling, inhibitory circuit development, nociceptive-system maturation, and the age-dependent actions of cytokines and BDNF may determine how the stimulus is encoded and later expressed in adult plasticity. These potential mechanisms provide a framework for interpreting the age-dependent findings and identifying targets for direct investigation in future studies. Additionally, it is important to acknowledge that this study evaluated exclusively male rats. Given the sex-dependent behavioral and neural consequences of early-life nociceptive stimulation (Lima et al. 2014; Malheiros et al. 2021), extending these investigations to female cohorts will help clarify the role of sex in the long-term modulation of dentate gyrus plasticity.

EPSP amplitude and slope reflect related aspects of synaptic activation, whereas PS reflects synchronous granule-cell firing and the conversion of synaptic input into population output (Bliss and

Gardner-Medwin 1973; Gilbert and Mack 1990; Frey et al. 1996; Bergado et al. 2009; Kenney and Manahan-Vaughan 2013; Lopez-Rojas and Kreutz 2016; Bronzino et al. 1994; Bliss et al. 2018). Absolute EPSP and slope did not differ among groups before or after HFS, but PS was higher in P8 than P1 at baseline and higher in P8 than CTR and P1 after HFS. This dissociation may reflect altered potentiation, EPSP–spike coupling, excitability, or spike recruitment. This pattern highlights a dissociation between synaptic responses and population output, motivating direct assessment of intrinsic excitability and inhibitory transmission to distinguish the contributions of the candidate mechanisms.

The layer-dependent effects further indicate that neonatal inflammatory pain did not alter the dentate gyrus uniformly. Instead, the consequences may depend on the synaptic pathway, local inhibitory control, and input–output organization examined. The molecular layer receives topographically organized perforant-path inputs from the medial and lateral entorhinal cortex, whereas recordings in the granule-cell layer emphasize population recruitment (Amaral et al. 2007; Witter 2007). Accordingly, reduced normalized molecular-layer potentiation and enhanced normalized granule-cell-layer slope potentiation in P1 may represent a circuit-selective redistribution of plasticity rather than contradictory effects. Baseline molecular-layer differences among groups, particularly in P8, provide an essential context for interpreting normalized post-HFS potentiation alongside absolute responses, integrating basal synaptic transmission with the relative magnitude of potentiation. Together, these complementary measures characterize the layer-dependent expression of dentate gyrus plasticity following neonatal inflammatory pain. This pattern motivates targeted investigation of pathway-specific synaptic plasticity and inhibitory regulation, as well as their potential implications for information processing in the dentate gyrus–CA3 network and pattern separation (Leutgeb et al. 2007).

The lower escape latencies in P1 and P8 on training days 3 and 4 indicate differences in water-maze acquisition performance, while probe-trial performance was comparable among groups. Hippocampal BDNF, a mediator of LTP maintenance and experience-dependent circuit remodeling (Bliss et al. 2018), was higher in P1 and P8 than in CTR and highest in P8. Neonatal noxious stimulation has likewise been associated with elevated BDNF and dentate cell proliferation (Malheiros et al. 2014). The increased BDNF levels provide molecular evidence of a lasting neurotrophic alteration associated with neonatal nociceptive experience, complementing the electrophysiological and behavioral findings. Together, these observations support investigating BDNF signaling as a candidate contributor to the long-term modifications in hippocampal function.

The concentration and volume of CFA shape the magnitude and duration of the neonatal inflammatory response. Here, plantar injection of 25 µL of the final 12.5% (v/v) CFA preparation produced a transient, localized inflammatory response that typically resolved within one week (Walker et al. 2003; Ren et al. 2004; Lima et al. 2014). Age-matched comparisons revealed a time- and exposure-age-dependent hippocampal cytokine profile: IL-6, IL-10, and TNF-α showed no CFA-related increases at D4 or D11, whereas IL-6 and IL-10 were lower in P1 than in controls at D30. At D30, P8 remained comparable to controls, and TNF-α did not differ among groups. These findings identify a later alteration in hippocampal cytokine levels following P1 stimulation, alongside the absence of detectable increases in the measured

cytokines at the sampled ages. Developmental variation in untreated controls further highlights the importance of age-matched comparisons for distinguishing treatment-associated changes from normal maturation. Together with previous studies using this protocol, these results support the lasting biological relevance of transient neonatal nociceptive exposure (Lima et al. 2014; Amaral et al. 2015; Malheiros et al. 2024). The comparison with handled controls characterizes the consequences of the neonatal inflammatory nociceptive procedure as a whole; separating the contributions of CFA, needle penetration, and other injection-related effects would require an additional saline-injected group.

Regarding the neuroimmune timeline, hippocampal cytokines were evaluated at selected developmental time points up to P30 to characterize their profile following neonatal CFA exposure and across the expected resolution of the peripheral inflammatory response (Lima et al. 2014). No CFA-related increases in hippocampal IL-6, IL-10, or TNF-α were detected at the evaluated time points, while IL-6 and IL-10 were lower in P1 than in age-matched controls at P30. This profile provides no support for sustained elevation of these cytokines through P30 and identifies a selective modification of hippocampal cytokine levels following P1 stimulation. Together with the adult electrophysiological findings, these results are consistent with lasting developmental effects of neonatal nociceptive exposure without detectable increases in the measured hippocampal cytokines at the sampled developmental stages.

Together, the findings support a working model in which the developmental timing of neonatal inflammatory nociceptive stimulation influences the maturation of neuroimmune signaling and hippocampal plasticity. Increased hippocampal BDNF in adult P1 and P8 rats provides molecular corroboration of a persistent neurodevelopmental alteration but does not establish BDNF as the mechanistic driver of the layer-specific electrophysiological or behavioral findings (Bliss et al. 2018; Malheiros et al. 2014). Because the present design did not include functional rescue, molecular knockdown, or pharmacological inhibition of BDNF–TrkB signaling, it cannot establish a causal pathway linking neonatal stimulation, adult BDNF availability, dentate gyrus potentiation, and water-maze performance. Cytokine-related developmental signaling may contribute to these long-term changes, but this possibility also remains hypothetical. Future studies using targeted manipulation of BDNF–TrkB signaling, combined with adult neuroimmune measurements and pathway-specific electrophysiological analyses, will be necessary to determine the causal relationships among these molecular, physiological, and behavioral outcomes.

Finally, a critical limitation of the present study is the exclusive use of male Wistar rats. Accumulating evidence indicates that neonatal pain experiences, neuroimmune signaling, and microglial activation trajectories exhibit pronounced sex-dependent profiles, often driven by distinct hormonal influences and differential neuroinflammatory responses during early development (LaPrairie and Murphy 2010; Lima et al. 2014; Malheiros et al. 2021, 2024). While our experimental design targeted male subjects to establish a rigorous, baseline characterization of layer-specific dentate gyrus plasticity and to ensure direct comparability with closely related historical datasets using the same neonatal CFA paradigm (Amaral et al. 2015; Malheiros et al. 2014), translating these neurodevelopmental findings to broader clinical

populations requires substantial caution. Consequently, evaluating these specific electrophysiological and molecular adaptations in female cohorts represents an essential and compelling direction for future research.

Conclusion

Neonatal inflammatory nociceptive stimulation was associated with persistent, layer-specific modification of adult dentate gyrus LTP and excitability. P1 showed greater normalized granule-cell-layer slope potentiation but lower normalized molecular-layer EPSP and slope potentiation than CTR, whereas P8 showed increased population-spike-related measures and lower normalized molecular-layer slope potentiation than CTR. Functionally, P1 and P8 showed shorter escape latencies than CTR on training days 3 and 4, although probe-trial performance did not differ. Increased hippocampal BDNF provided molecular corroboration. No increases in hippocampal IL-6, IL-10, or TNF-α were detected up to P30, while reduced thermal sensitivity documented a lasting sensory consequence of the model. Together, these findings support developmental-stage-dependent reorganization of adult dentate gyrus function without establishing a causal pathway among the electrophysiological, behavioral, and molecular outcomes.

Declarations

Institutional Review Board Statement

The study was approved by the Ethics Committee of the Federal University of São João del-Rei under protocol number 024/2016. All efforts were made to minimize animal suffering.

Conflicts of Interest:

The authors declare no conflicts of interest. The funding agencies provided financial support only, with no role in the study or publication process.

Author Contribution

This study was designed by L.C. and A.-C.G.A. The experiments were performed by L.N.C.B., G.S.N., A.C.P., and A.M.R. Data were curated by L.N.C.B., G.S.N., A.M.R. and A.C.P. The data were analyzed by A.M.R., A.C.P., F.A.S. and C.A.S., and the results were critically examined by all authors. A.M.R. had a primary role in preparing the manuscript, with substantial contributions from L.C. and A.-C.G.A. The manu-script was reviewed and edited by C.A.S., F.A.S., and L.C. L.C. and A.-C.G.A. supervised the study and provided methodological support and resources. All authors have approved the final version of the manuscript and agree to be accountable for all aspects of the work.

Acknowledgement

This work was supported by the Brazilian agencies: Fundação de Amparo à Pesquisa de Minas Gerais (FAPEMIG), Fundação de Amparo à Pesquisa do Estado de São Paulo (FAPESP), Conselho Nacional de Desenvolvimento Científico e Tecnológico (CNPq), Programa de Excelência Acadêmica / Coordenação de Aperfeiçoamento de Pessoal de Nível Superior (PROEX/CAPES), Laboratório Nacional para Estudo do Cálcio Celular (LABNECC/FINEP) and Instituto Nacional de Neurociência Translacional (INNT) (Ministério da Ciência e Tecnologia/CNPq/FAPESP).

Data Availability Statement

The data that support the findings of this study are available from the corresponding author upon reasonable request.

Abbreviations

NICUs	Neonatal Intensive Care Units
P	Postnatal day
CNS	Central Nervous system
LTP	Long-Term Potentiation
CFA	Complete Freund's Adjuvant
CTR	Control Group
HFS	High Frequency Stimulation
TBS	Theta-Burst Stimulation
EP	Extracellular Potential
EPSP	Excitatory Postsynaptic Potential

References

1. Adamson WT, Windh RT, Blackford S, Kuhn CM (1991) Ontogeny of μ- and κ-opiate receptor control of the hypothalamo-pituitary-adrenal axis in rats. Endocrinology 129:959–964. https://doi.org/10.1210/endo-129-2-959
2. Almeida ACA, Rodrigues AM, Scorza FA, Cavalheiro EA, Teixeira HZ, Duarte MA, Silveira GA, Arruda EZ (2008) Mechanistic hypotheses for nonsynaptic epileptiform activity induction and its transition

from the interictal to ictal state—computational simulation. Epilepsia 49:1908–1924. https://doi.org/10.1111/j.1528-1167.2008.01686.x

3. Altman J, Das G (1965) Autoradiographic and histological evidence of postnatal hippocampal neurogenesis in rats. J Comp Neurol 124:319–335. https://doi.org/10.1002/cne.901240303
4. Amaral C, Antonio B, Oliveira MGM, Hamani C, Guinsburg R, Covolan L (2015) Early postnatal nociceptive stimulation results in deficits of spatial memory in male rats. Neurobiol Learn Mem 125:120–125. https://doi.org/10.1016/j.nlm.2015.08.012
5. Amaral DG, Scharfman HE, Lavenex P (2007) The dentate gyrus: Fundamental neuroanatomical organization (dentate gyrus for dummies). Prog Brain Res 163:3–22. https://doi.org/10.1016/S0079-6123(07)63001-5
6. Anand KJS (1998) Clinical importance of pain and stress in preterm neonates. Biol Neonate 73:1–9. https://doi.org/10.1159/000013953
7. Anand KJS, Scalzo FM (2000) Can adverse neonatal experiences alter brain development and subsequent behavior? Biol Neonate 77:69–82. https://doi.org/10.1159/000014197
8. Anand KJ, Carr DB (1989) The neuroanatomy, neurophysiology, and neurochemistry of pain, stress, and analgesia in newborns and children. Pediatr Clin North Am 36:795–822. https://doi.org/10.1016/S0031-3955(16)36722-0
9. Anand KJ, Coskun V, Thrivikraman K, Nemeroff C, Plotsky P (1999) Long-term behavioral effects of repetitive pain in neonatal rat pups. Physiol Behav 66:627–637. https://doi.org/10.1016/S0031-9384(98)00338-2
10. Beggs S, Currie G, Salter MW, Fitzgerald M, Walker SM (2012) Priming of adult pain responses by neonatal pain experience: Maintenance by central neuroimmune activity. Brain 135:404–417. https://doi.org/10.1093/brain/awr288
11. Bergado JA, Scherf T, Almaguer-Melian W, Frey S, Lopez J, Frey JU (2009) Stimulation of the nucleus raphe medialis modifies basal synaptic transmission at the dentate gyrus, but not long-term potentiation or its reinforcement by stimulation of the basolateral amygdala. Neurosci Lett 464:179–183. https://doi.org/10.1016/j.neulet.2009.08.034
12. Bernardi M, Genedani S, Bertolini A (1986) Behavioral activity and active avoidance learning and retention in rats neonatally exposed to painful stimuli. Physiol Behav 36:553–555. https://doi.org/10.1016/0031-9384(86)90330-6
13. Bhutta AT, Rovnahi C, Simpson PM, Gossett JM, Scalzo FM, Anand KJS (2001) Interactions of inflammatory pain and morphine in infant rats: Long-term behavioral effects. Physiol Behav 73:51–58. https://doi.org/10.1016/S0031-9384(01)00432-2
14. Bliss TVP, Collingridge GL (1993) A synaptic model of memory: Long-term potentiation in the hippocampus. Nature 361:31–39. https://doi.org/10.1038/361031a0
15. Bliss TVP, Collingridge GL, Borris RGM, Reymann KG (2018) Long-term potentiation in the hippocampus: Discovery, mechanisms and function. Neuroforum 24:A1–A18. https://doi.org/10.1515/nf-2017-A059

16. Bliss TV, Gardner-Medwin AR (1973) Long-lasting potentiation of synaptic transmission in the dentate area of the unanaesthetized rabbit following stimulation of the perforant path. J Physiol 232:357–374. https://doi.org/10.1113/jphysiol.1973.sp010274
17. Bliss TV, Lømo T (1973) Long-lasting potentiation of synaptic transmission in the dentate area of the anesthetized rabbit following stimulation of the perforant path. J Physiol 232:331–356. https://doi.org/10.1113/jphysiol.1973.sp010273
18. Bronzino JD, Abu-Hasaballah K, Austin-LaFrance RJ, Morgane PJ (1994) Maturation of long-term potentiation in the hippocampal dentate gyrus of the freely moving rat. Hippocampus 4:439–446. https://doi.org/10.1002/hipo.450040406
19. Brunson KL, Eghbal-Ahmadi M, Bender R, Chen Y, Baram TZ (2001) Long-term, progressive hippocampal cell loss and dysfunction induced by early-life administration of corticotropin-releasing hormone reproduce the effects of early-life stress. Proc Natl Acad Sci USA 98:8856–8861. https://doi.org/10.1073/pnas.151224898
20. Brunson KL, Kramár E, Lin B, Chen Y, Colgin LL, Yanagihara TK, Lynch G, Baram TZ (2005) Mechanisms of late-onset cognitive decline after early-life stress. J Neurosci 25:9328–9338. https://doi.org/10.1523/JNEUROSCI.2281-05.2005
21. Cooke S, Bliss T (2006) Plasticity in the human central nervous system. Brain 129:1659–1673. https://doi.org/10.1093/brain/awl082
22. Covolan L, de Almeida ACG, Amorim B, Cavarsan C, Miranda MF, Aarão MC, Madureira AP, Rodrigues AM, Nobrega JN, Mello LE, Hamani C (2014) Effects of anterior thalamic nucleus deep brain stimulation in chronic epileptic rats. PLoS ONE 9:e97618. https://doi.org/10.1371/journal.pone.0097618
23. Fitzgerald M, Shaw A, MacIntosh N (1988) Postnatal development of the cutaneous flexor reflex: Comparative study of preterm infants and newborn rat pups. Dev Med Child Neurol 30:520–526. https://doi.org/10.1111/j.1469-8749.1988.tb04779.x
24. Frey U, Frey S, Schollmeier F, Krug M (1996) Influence of actinomycin D, a RNA synthesis inhibitor, on long-term potentiation in rat hippocampal neurons in vivo and in vitro. J Physiol 490:703–711. https://doi.org/10.1113/jphysiol.1996.sp021179
25. Gilbert ME, Mack CM (1990) The NMDA antagonist MK-801 suppresses long-term potentiation, kindling, and kindling-induced potentiation in the perforant path of the unanesthetized rat. Brain Res 519:89–96. https://doi.org/10.1016/0006-8993(90)90064-I
26. Grunau RE, Haley DW, Whitfield MF, Weinberg J, Yu W, Thiessen P (2007) Altered basal cortisol levels at 3, 6, 8 and 18 months in infants born at extremely low gestational age. J Pediatr 150:151–156. https://doi.org/10.1016/j.jpeds.2006.10.053
27. Grunau R, Holsti L, Peters J (2006) Long-term consequences of pain in human neonates. Semin Fetal Neonatal Med 11:268–275. https://doi.org/10.1016/j.siny.2006.02.007
28. Guy ER, Abbott FV (1992) The behavioral response to formalin pain in preweanling rats. Pain 51:81–90. https://doi.org/10.1016/0304-3959(92)90012-Z

29. Hohmann AG, Neely MH, Piña J, Nackley AG (2005) Neonatal chronic hind paw inflammation alters sensitization to intradermal capsaicin in adult rats: a behavioral and immunocytochemical study. J Pain 6:798–808. https://doi.org/10.1016/j.jpain.2005.07.009
30. Joëls M, Karst H, Alfarez D, Heine VM, Qin Y, van Riel E, Verkuyl M, Lucassen PJ, Krugers HJ (2004) Effects of chronic stress on structure and cell function in rat hippocampus and hypothalamus. Stress 7:221–231. https://doi.org/10.1080/10253890500070005
31. Johnston C, Stevens B, Craig K, Grunau R (1993) Developmental changes in pain expression in premature, full-term, two- and four-month-old infants. Pain 52:201–208. https://doi.org/10.1016/0304-3959(93)90132-9
32. Kenney J, Manahan-Vaughan D (2013) NMDA receptor-dependent synaptic plasticity in dorsal and intermediate hippocampus exhibits distinct frequency-dependent profiles. Neuropharmacology 74:108–118. https://doi.org/10.1016/j.neuropharm.2013.02.017
33. Kim J, Foy M, Thompson R (1996) Behavioral stress modifies hippocampal plasticity through N-methyl-D-aspartate receptor activation. Proc Natl Acad Sci USA 93:4750–4753. https://doi.org/10.1073/pnas.93.10.4750
34. LaPrairie J, Murphy A (2010) Long-term impact of neonatal injury in male and female rats: Sex differences, mechanisms and clinical implications. Front Neuroendocrinol 31:193–202. https://doi.org/10.1016/j.yfrne.2010.02.001
35. Leslie ATFS, Akers KG, Martinez-Canabal A, Mello LEA, Covolan L, Guinsburg R (2011) Neonatal inflammatory pain increases hippocampal neurogenesis in rat pups. Neurosci Lett 501:78–82. https://doi.org/10.1016/j.neulet.2011.06.047
36. Leutgeb JK, Leutgeb S, Moser MB, Moser EI (2007) Pattern separation in the dentate gyrus and CA3 of the hippocampus. Science 315:961–966. https://doi.org/10.1126/science.1135801
37. Lidow MS (2002) Long-term effects of neonatal pain on nociceptive systems. Pain 99:377–383. https://doi.org/10.1016/S0304-3959(02)00258-0
38. Lima M, Malheiros J, Negrigo A, Tescarollo F, Medeiros M, Suchecki D, Tannús A, Guinsburg R, Covolan L (2014) Sex-related long-term behavioral and hippocampal cellular alterations after nociceptive stimulation throughout postnatal development in rats. Neuropharmacology 77:268–276. https://doi.org/10.1016/j.neuropharm.2013.10.007
39. Lopez-Rojas J, Kreutz MR (2016) Mature granule cells of the dentate gyrus—Passive bystanders or principal performers in hippocampal function? Neurosci Biobehav Rev 64:167–174. https://doi.org/10.1016/j.neubiorev.2016.02.021
40. Lupien SJ, McEwen BS, Gunnar MR, Heim C (2009) Effects of stress throughout the lifespan on the brain, behaviour and cognition. Nat Rev Neurosci 10:434–445. https://doi.org/10.1038/nrn2639
41. Malheiros JM, Andreeta MB, Polli RS, Paiva FF, Tannús A, Guinsburg R, Covolan L (2021) Adult brain activation in response to pain is changed by neonatal painful stimulation according to sex: A manganese-enhanced MRI study. Eur J Neurosci 53:571–587. https://doi.org/10.1111/ejn.14948

42. Malheiros JM, Lima M, Avanzi RDT, Silva SG, Suchecki D, Guinsburg R, Covolan L (2014) Repetitive noxious neonatal stimuli increases dentate gyrus cell proliferation and hippocampal brain-derived neurotrophic factor levels. Hippocampus 24:415–423. https://doi.org/10.1002/hipo.22235
43. Malheiros J, Amaral C, Silva LS, Guinsburg R, Covolan L (2024) Neonatal nociceptive stimulation results in pain sensitization, reduction of hippocampal 5-HT1A receptor, and p-CREB expression in adult female rats. Behav Brain Res 466:114975. https://doi.org/10.1016/j.bbr.2024.114975
44. Negrigo A, Medeiros M, Guinsburg R, Covolan L (2011) Long-term gender behavioral vulnerability after nociceptive neonatal formalin stimulation in rats. Neurosci Lett 490:196–199. https://doi.org/10.1016/j.neulet.2010.12.050
45. Pavlides C, Nivón LG, McEwen B (2002) Effects of chronic stress on hippocampal long-term potentiation. Hippocampus 12:245–257. https://doi.org/10.1002/hipo.1116
46. Rêgo DSB, Silva CS, Mello LEAM, Leslie ATFS (2022) Early life nociceptive stimulus and fentanyl exposure increase hippocampal neurogenesis and anxiety but do not affect spatial learning and memory. Front Neurosci 16:988096. https://doi.org/10.3389/fnins.2022.988096
47. Ren K, Anseloni V, Zou P, Wade EB, Novikova SI, Ennis M, Traub RJ, Gold MS, Dubner R, Lidow MS (2004) Characterization of basal and re-inflammation-associated long-term alteration in pain responsivity following short-lasting neonatal local inflammatory insult. Pain 110:588–596. https://doi.org/10.1016/j.pain.2004.04.006
48. Ruda MA, Ling QD, Hohmann AG, Peng YB, Tachibana T (2000) Altered nociceptive neuronal circuits after neonatal peripheral inflammation. Science 289:628–630. https://doi.org/10.1126/science.289.5479.628
49. Schneiderman N, Spear NE, Spear LP (2003) Developmental psychobiology: an interdisciplinary science, 1st edn. MIT Press, Cambridge, pp 413–416
50. Unruh AM (1996) Gender variations in clinical pain experience. Pain 65:123–167. https://doi.org/10.1016/0304-3959(95)00214-6
51. Walker CD, Deschamps S, Proulx K, Tu M, Salzman C, Woodside B, Lupien S, Gallo-Payet N, Richard D (2004) Mother to infant or infant to mother? Reciprocal regulation of responsiveness to stress in rodents and the implications for humans. J Psychiatry Neurosci 29:364–382
52. Walker SM, Meredith-Middleton J, Cooke-Yarborough C, Fitzgerald M (2003) Neonatal inflammation and primary afferent terminal plasticity in the rat dorsal horn. Pain 105:185–195. https://doi.org/10.1016/S0304-3959(03)00201-X
53. Witter MP (2007) The perforant path: Projections from the entorhinal cortex to the dentate gyrus. Prog Brain Res 163:43–61. https://doi.org/10.1016/S0079-6123(07)63003-9
54. Zoghbi HY, Bear MF (2012) Synaptic dysfunction in neurodevelopmental disorders associated with autism and intellectual disabilities. Cold Spring Harb Perspect Biol 4:a009886. https://doi.org/10.1101/cshperspect.a009886

Figures

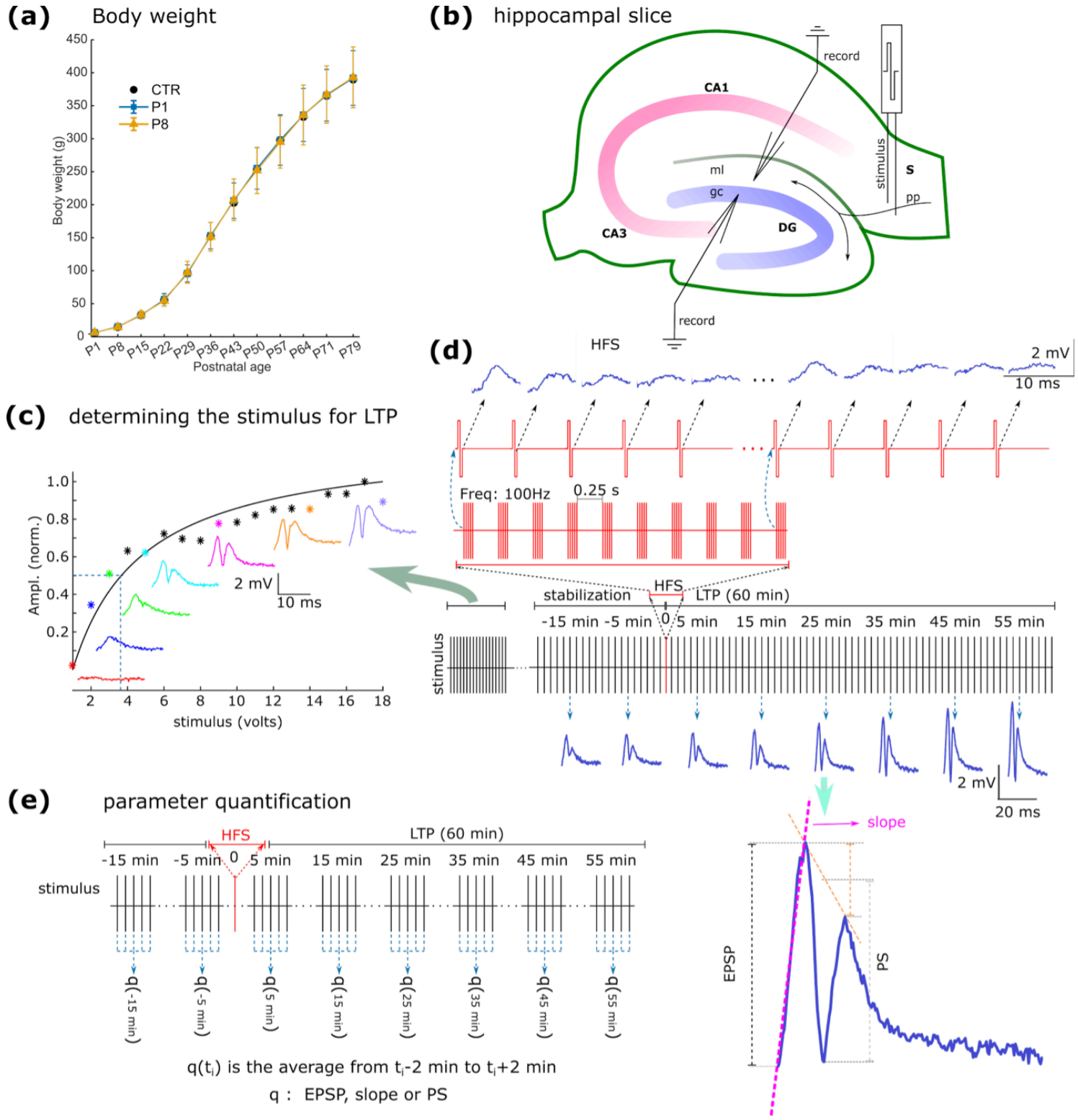


Figure 1

Body weight and detailed description of the electrophysiological procedure used to induce LTP. (A) Body weight of animals in the control (CTR), P1, and P8 groups as a function of postnatal age, from P1 to P79. Data are presented as mean ± SEM. Circles, squares, and triangles represent the CTR, P1, and P8 groups, respectively. (B) Schematic representation of the hippocampal slice indicating the regions used for extracellular potential recordings and the positioning of the stimulation electrode in the perforant path.

(C) Procedure used to determine the stimulus intensity applied in each experiment, corresponding to 50% of the intensity required to evoke the maximal response. This procedure was performed for each hippocampal slice at the beginning of the experiment. (D) Temporal stimulation protocol used to induce and record LTP. After determining the stimulation intensity, stimuli were delivered every 60 s for approximately 20 min to stabilize baseline responses. High-frequency stimulation (HFS), defined as t = 0, was then applied. Following HFS, stimuli were delivered every 60 s for an additional 60 min. Representative responses recorded throughout the LTP procedure are shown. (E) Schematic illustration of the parameters used to quantify LTP in each experimental group.

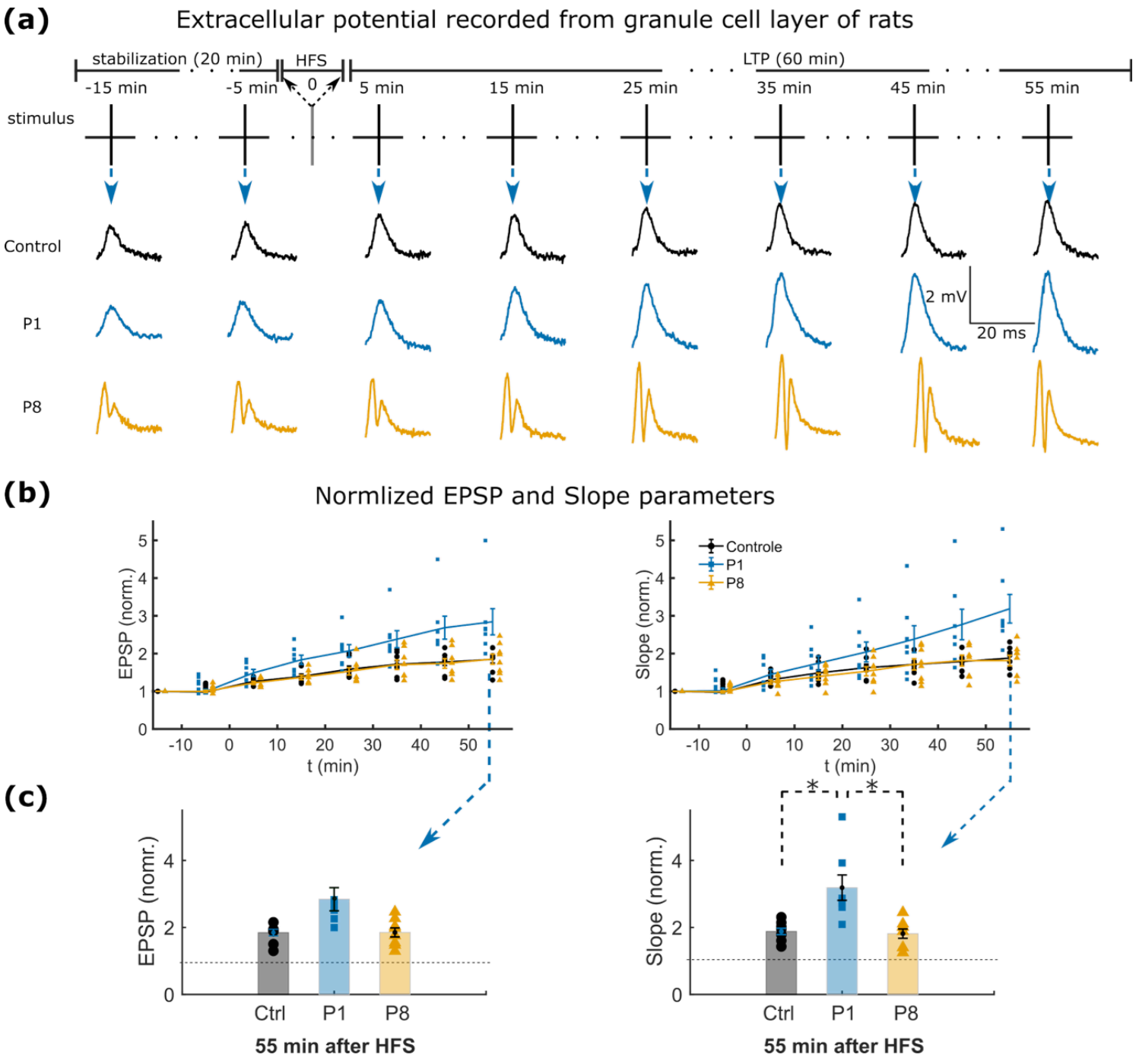


Figure 2

LTP induced in the dentate gyrus (DG) of male rats, observed by extracellular recordings obtained from the granule-cell layer. (**a**) Representative population potentials illustrating response potentiation in the granule cell layer. (**b**) EPSP and slope parameters normalized to baseline values recorded before HFS (t = -15 min). (**c**) Comparison among Control (CTR, n = 8), P1 (n = 7), and P8 (n = 8) groups. According to the Kruskal-Wallis test followed by Dunn-Bonferroni post hoc comparisons, normalized EPSP potentiation did not differ significantly among groups: H(2) = 5.161, P = 0.0757, q = 0.0757 (CTR vs. P1, P = 0.1401; CTR vs. P8, P = 1.0; P1 vs. P8, P = 0.1401). Normalized slope potentiation differed significantly among groups: H(2) = 13.615, P = 0.0011, q = 0.0044 (CTR vs. P1, P = 0.0022; CTR vs. P8, P = 1.0; P1 vs. P8, P = 0.0067). The P1 group showed greater slope potentiation than CTR and P8 ("*" indicates statistical significance).

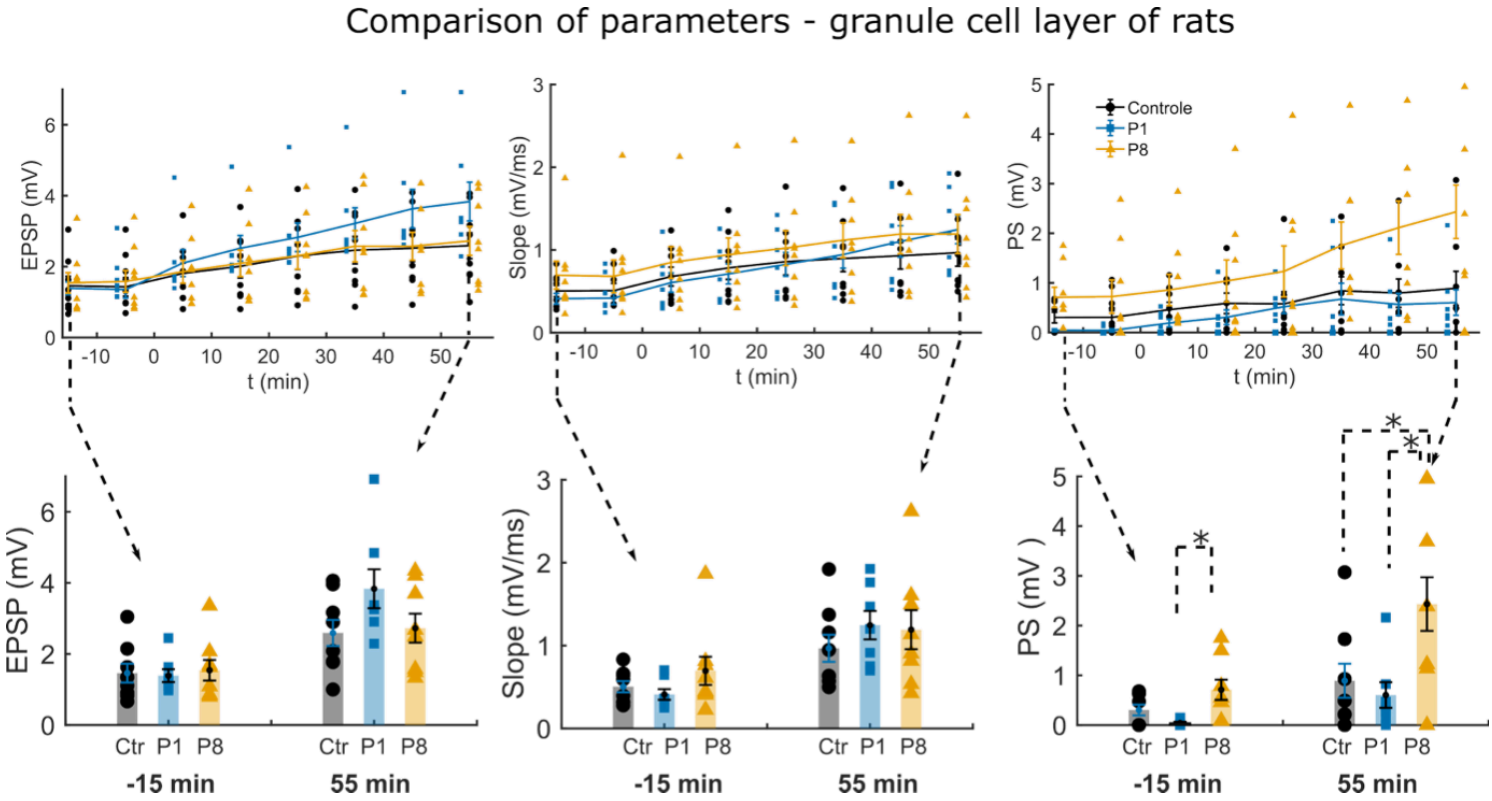


Figure 3

Estimation of EPSP, slope, and PS parameters from population potentials recorded in the granule-cell layer of the DG of male rats (top panel). Comparisons were performed between values obtained before (t = -15 min) and after (t = 55 min) HFS, where "*" indicates a statistical significance, according to the Kruskal-Wallis test followed by the Dunn-Bonferroni test. EPSP: t = -15 min, H(2) = 0.077, P = 0.9623, q = 0.9623; t = 55 min, H(2) = 3.068, P = 0.2156, q = 0.2875. Slope: t = -15 min, H(2) = 2.459, P = 0.2924, q = 0.3509; t = 55 min, H(2) = 1.491, P = 0.4746, q = 0.5177. PS: t = -15 min, H(2) = 7.270, P = 0.0264, q = 0.0396 (CTR vs. P1, P = 0.7525; CTR vs. P8, P = 0.3414; P1 vs. P8, P = 0.0223); t = 55 min, H(2) = 10.195, P = 0.0061, q = 0.0122 (CTR vs. P1, P = 1.0; CTR vs. P8, P = 0.0364; P1 vs. P8, P = 0.0084).

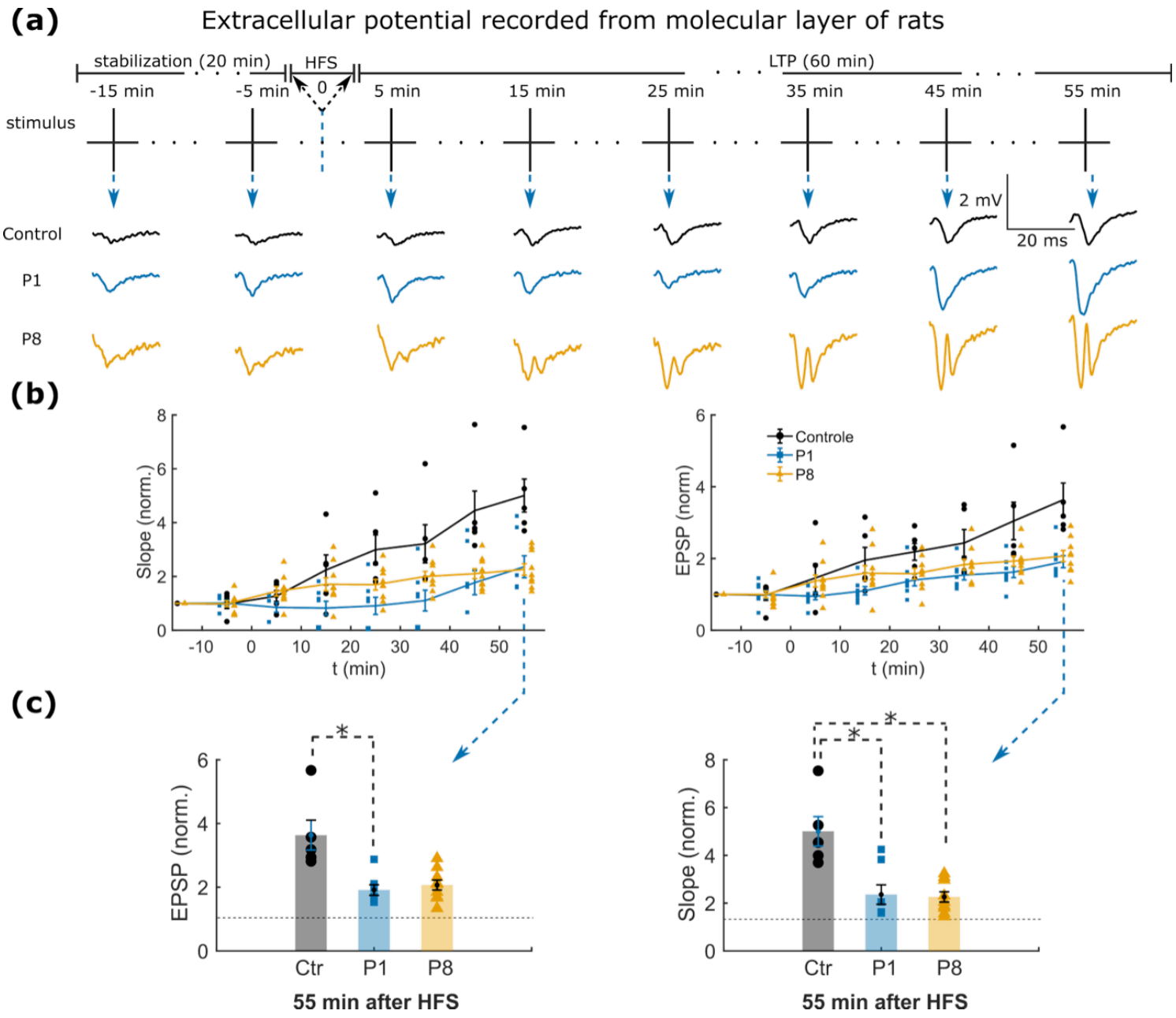


Figure 4

LTP induced in the DG of male rats, assessed by extracellular recordings obtained from the molecular layer. (**a**) Representative population potentials illustrating response potentiation in the molecular layer. (**b**) EPSP and slope parameters normalized to baseline values recorded before HFS (t=-15 min). (**c**) Comparison among Control (n = 6), P1 (n = 7), and P8 (n = 9) groups. According to the Kruskal-Wallis test followed by Dunn-Bonferroni post hoc comparisons, normalized EPSP differed significantly among groups: H(2) = 7.140, P = 0.0282, q = 0.0376 (CTR vs. P1, P = 0.0271; CTR vs. P8, P = 0.1216; P1 vs. P8, P = 1.0). Normalized slope also differed significantly among groups: H(2) = 7.911, P = 0.0192, q = 0.0376 (CTR vs. P1, P = 0.0368; CTR vs. P8, P = 0.0327; P1 vs. P8, P = 1.0). CTR showed greater slope potentiation than P1 and P8, but greater EPSP potentiation only in comparison with P1 ("*" indicates statistical significance).

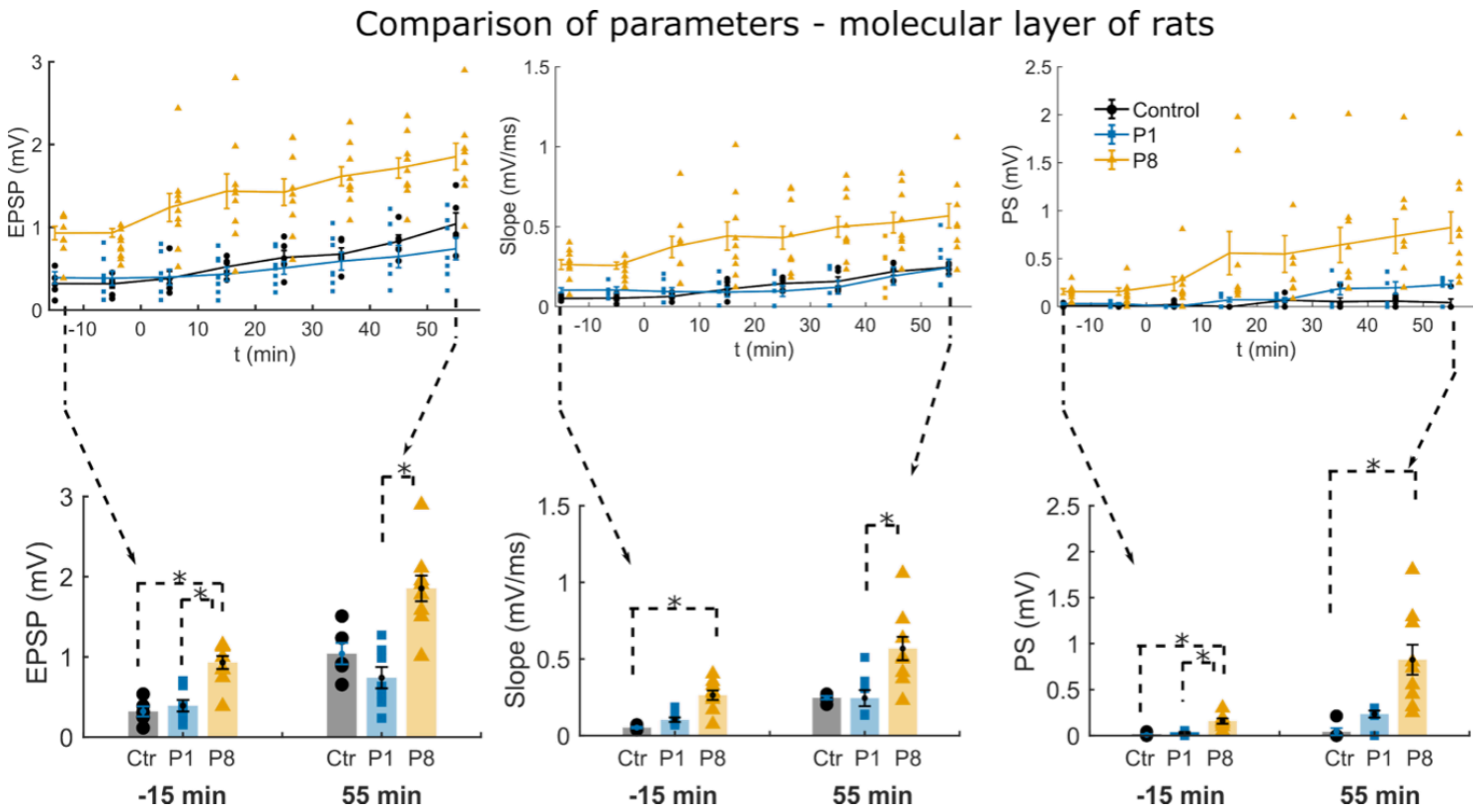


Figure 5

EPSP, slope, and PS parameters from population potentials recorded in the molecular layer of the DG of male rats (top panel). Comparisons were performed between values obtained before (t=-15 min) and after (t=55 min) HFS. "*" indicates statistical significance according to the Kruskal-Wallis test followed by Dunn-Bonferroni post hoc comparisons. EPSP: t = -15 min, H(2) = 12.321, P = 0.0021, q = 0.0050 (CTR vs. P1, P = 1.0; CTR vs. P8, P = 0.0076; P1 vs. P8, P = 0.0136); t = 55 min, H(2) = 12.765, P = 0.0017, q = 0.0050 (CTR vs. P1, P = 1.0; CTR vs. P8, P = 0.0701; P1 vs. P8, P = 0.0018). Slope: t = -15 min, H(2) = 14.609, P = 0.0007, q = 0.0044 (CTR vs. P1, P = 0.1981; CTR vs. P8, P = 0.0005; P1 vs. P8, P = 0.1234); t = 55 min, H(2) = 9.858, P = 0.0072, q = 0.0123 (CTR vs. P1, P = 1.0; CTR vs. P8, P = 0.0577; P1 vs. P8, P = 0.0132). PS: t = -15 min, H(2) = 13.594, P = 0.0011, q = 0.0044 (CTR vs. P1, P = 0.8400; CTR vs. P8, P = 0.0016; P1 vs. P8, P = 0.0280); t = 55 min, H(2) = 13.952, P = 0.0009, q = 0.0044 (CTR vs. P1, P = 0.2930; CTR vs. P8, P = 0.0007; P1 vs. P8, P = 0.0896).

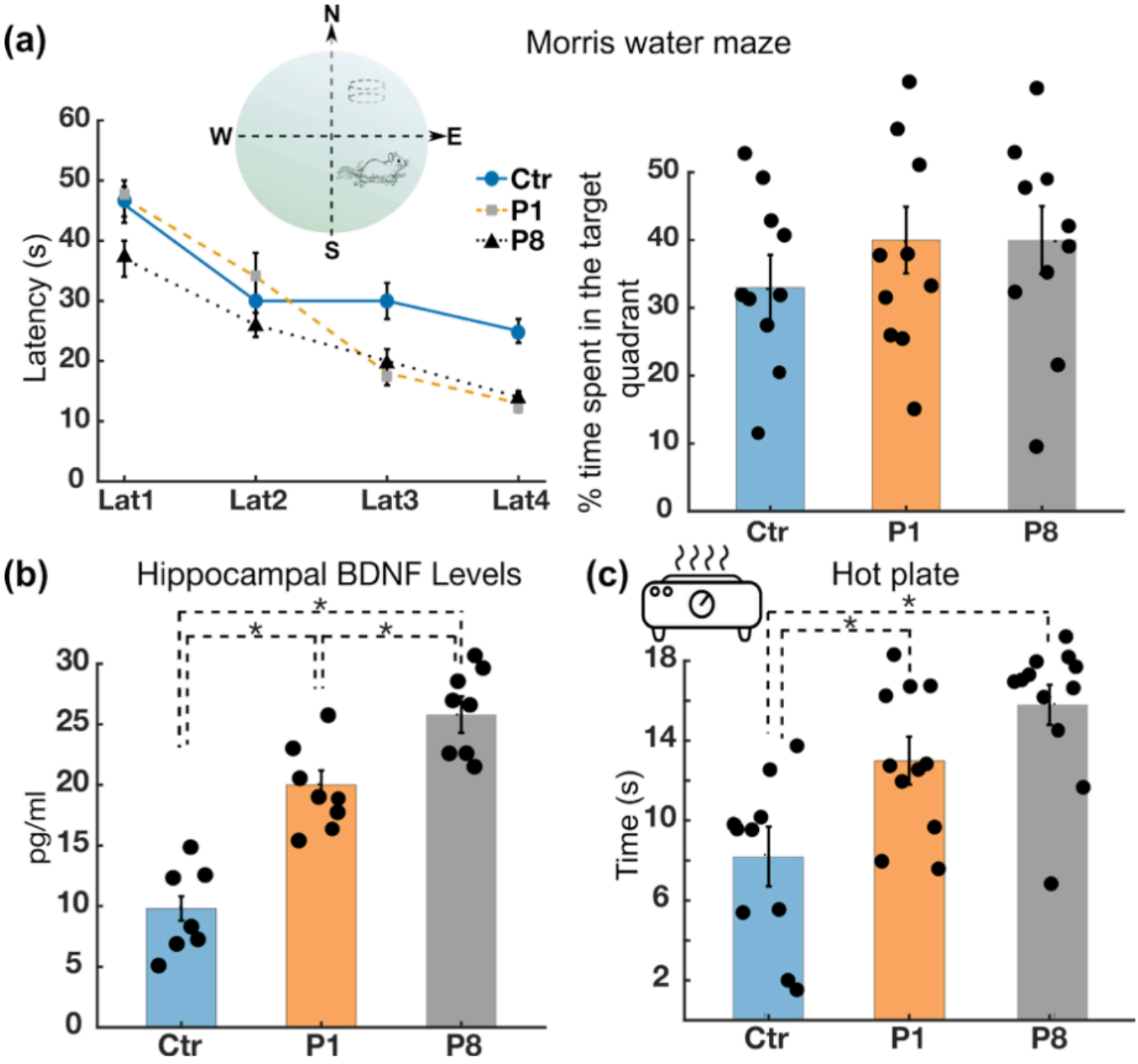


Figure 6

Behavioral data and hippocampal BDNF concentrations. (**a**) Morris water-maze performance (CTR, n = 10; P1, n = 10; P8, n = 10). Three animals—two CTR and one P1—were excluded because marked agitation and stress responses prevented valid task performance. Left: escape latency during training days 1–4. Right: percentage of time spent in the target quadrant during the probe trial on day 5. (**b**) Hippocampal BDNF concentrations (CTR, n = 7; P1, n = 8; P8, n = 8). (**c**) Hot-plate test. Paw-withdrawal latency at 52.5 °C in adult rats (CTR, n = 10; P1, n = 11; P8, n = 12). Data are presented as mean ± SEM; individual values are overlaid for the hot-plate, probe-trial, and BDNF panels. Bonferroni-adjusted pairwise comparisons were significant for CTR versus P1 and CTR versus P8 in the hot-plate test, and for

all three pairwise comparisons of BDNF concentrations. Water-maze acquisition was evaluated using day-specific comparisons. Across the two adult behavioral endpoints, the omnibus hot-plate effect remained significant after FDR adjustment (q = 0.00046), whereas the probe-trial effect did not (q = 0.800). Day-specific ANOVAs, adjusted across the four training days using the Holm procedure, showed no significant group effect on day 1 ($F(2,27) = 3.37$, Holm-adjusted P = 0.099) or day 2 ($F(2,27) = 1.49$, Holm-adjusted P = 0.243), but significant group effects on day 3 ($F(2,27) = 7.29$, Holm-adjusted P = 0.0088) and day 4 ($F(2,27) = 18.34$, Holm-adjusted P < 0.001). On day 3, Bonferroni-adjusted pairwise comparisons showed longer escape latency in CTR than in P1 (P = 0.0083) and P8 (P = 0.037). On day 4, escape latency was also longer in CTR than in P1 and P8 (both P < 0.001). P1 and P8 did not differ on either day.

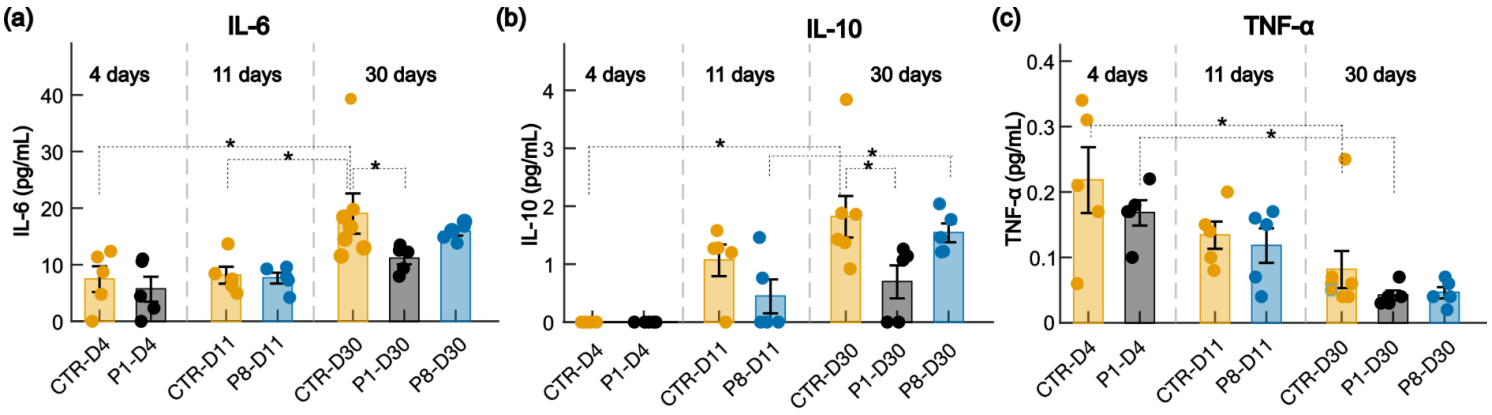


Figure 7

Hippocampal cytokine concentrations following neonatal inflammatory nociceptive stimulation. Levels of IL-6 (**a**), IL-10 (**b**), and TNF-α (**c**) were quantified in the hippocampus 3 days after neonatal CFA administration (P1-D4 and P8-D11) and on postnatal day 30 (P1-D30 and P8-D30). Age-matched comparisons at D4 and D11 were performed using two-sided Mann–Whitney tests with exact permutation P values. At D4, no differences were detected between CTR-D4 and P1-D4 for IL-6 (U = 8.5, P = 0.4603, q = 0.8214), IL-10 (P = 1.0000, q = 1.0000), or TNF-α (U = 9.0, P = 0.5476, q = 0.8214). At D11, no differences were detected between CTR-D11 and P8-D11 for IL-6 (U = 12.0, P = 1.0000, q = 1.0000), IL-10 (U = 6.5, P = 0.2381, q = 0.7143), or TNF-α (U = 11.5, P = 0.8810, q = 1.0000). At D30, Kruskal–Wallis tests showed FDR-significant group effects for IL-6, $H(2) = 7.511$, P = 0.0234, q = 0.0458, and IL-10, $H(2) = 6.980$, P = 0.0305, q = 0.0458, but not TNF-α, $H(2) = 2.842$, P = 0.2414, q = 0.2414. Dunn–Bonferroni comparisons showed lower IL-6 (P = 0.0390) and IL-10 (P = 0.0410) in P1-D30 than in CTR-D30; all other D30 comparisons were nonsignificant. Data are displayed as mean ± SEM with individual values overlaid (n = 5 per group, except CTR-D30, n = 7); statistical analyses were nonparametric. Temporal comparisons within experimental condition showed the following significant differences: CTR-D30 versus CTR-D4 for IL-6 (P = 0.0211), IL-10 (P = 0.0031), and TNF-α (P = 0.0372); CTR-D30 versus CTR-D11 for IL-6 (P = 0.0313); P1-D30 versus P1-D4 for TNF-α (U = 0.0, P = 0.0079); and P8-D30 versus P8-D11 for IL-6 (U = 0.0, P = 0.0079) and IL-10 (U = 2.5, P = 0.0397). All other temporal comparisons were nonsignificant.